

# Open-path Fourier transform infrared spectrometry characterization of low temperature combustion gases in biomass fuels

A.J. de Castro <sup>a,\*</sup>, A.M. Lerma <sup>a</sup>, F. López <sup>a</sup>, M. Guijarro <sup>b</sup>, C. Díez <sup>b</sup>,  
C. Hernando <sup>b</sup>, J. Madrigal <sup>b</sup>

<sup>a</sup> LIR-Dept. de Física, Universidad Carlos III de Madrid, Avda Universidad 30, 28911-Leganés, Madrid, Spain

<sup>b</sup> CIFOR-INIA, Laboratorio de Incendios Forestales, P.O. Box 8111, 28080 Madrid, Spain

Received 10 April 2006

Available online 22 January 2007

## Abstract

Accurate determination of gas concentration emitted during thermal degradation (pyrolysis) of biomass in forest fires is one of the keypoints in recent research on physical-based fire spread models. However, it is a very cumbersome task not well solved by classical invasive sensors and procedures. In this work, a methodology to use open-path Fourier transform-based infrared (OP-FTIR) spectrometry has been applied as a remote sensing technique that permits in situ, non-intrusive and simultaneous measurements. Main gaseous by-products (CO, CO<sub>2</sub>, CH<sub>4</sub> and NH<sub>3</sub>) have been measured and quantified in terms of path-integrated concentrations. Different emission ratios have been determined for the species under study. These results can help to simplify the modelling of pyrolysis processes inside the physical-based models for fire spread.

© 2006 Elsevier B.V. All rights reserved.

*Keywords:* Open-path FTIR; Pyrolysis; Quantitative analysis; Wildland fire models

## 1. Introduction

Physical models for predicting wildland fire behaviour are based on the resolution of a set of conservation equations (mass, momentum and energy) in order to estimate the energy flux between burning and unburned fuel [1]. One of the keypoints of these models concerns the modelling of the thermal degradation of biomass (pyrolysis). This complex process generates different gases, some of them flammables, acting ahead the fire on the rate of spread. Experimental knowledge of these gas concentrations is a determinant factor to validate and improve these models trying to simulate the spread of a fire. However, one important problem is to perform an accurate mode to measure the concentration of pyrolysis gases as they are produced in a harsh environment and at open air.

This paper presents an experimental characterization of gases emitted during thermal degradation of selected Galician shrub fuels. The work has been divided in different parts. The first one focuses on the experimental setup and the preparation of samples. This is an important part of the work as it makes feasible comparisons between IR procedures and classical forest ones. The second part of this work is devoted to the experimental results and the analysis of correlations between the concentrations of different pyrolysis gases for the species under study. Finally, some conclusions about these results and further applications are proposed.

### 1.1. Thermal degradation of biomass

Wood (and, in general, forest fuels) is a thermally degradable and combustible material mainly composed by cellulose (~40%), hemicellulose (~30%) and lignin (~25%). A small proportion is solvent soluble extractives

\* Corresponding author. Fax: +34 91 624 8749.

E-mail address: [decastro@fis.uc3m.es](mailto:decastro@fis.uc3m.es) (A.J. de Castro).

(lipids and terpenes) and inorganic materials (ashes) [2]. When wood temperature is increased, the different chemical components undergo a thermal degradation. This thermal degradation is called pyrolysis. The process is very complex, and can be divided in different temperature regimes.

A general description of the process can be found in Ref. [3]. Below 100 °C only the loss of water is remarkable. Between 100 °C and 200 °C water vapour and other non-combustible gases like carbon dioxide, formic acid and acetic acid are produced. Exothermic oxidation reactions can occur because ambient air can diffuse into and react with the developing char residue. From 200 °C to 300 °C active pyrolysis begins with the decomposition of hemicellulose and lignin. The same gases cited previously are produced, but with a greatly reduced quantity of water vapour and now significant amounts of carbon monoxide are emitted. At this point, the products are almost entirely non-flammable. From 300 °C to 500 °C the rapid decomposition of cellulose takes place giving rise to an important production of flammable volatiles and tars. If these gases are mixed with air and heated to their ignition temperature, transition to flaming combustion (fast exothermic gas-phase reactions that emit radiation in the visible spectrum) can occur. Above 500 °C all volatiles are gone, and the remaining wood residue is char that can be oxidized to CO<sub>2</sub>, CO and H<sub>2</sub>O (glowing combustion).

## 2. Experimental description

### 2.1. Samples

Over 14,000 wildfires happen every year in Galicia (NW of Spain) and more than 80% of them burn in shrubland areas [4] where different shrubs communities (gorse, winged broom, heather, etc.) are widespread. The study of initial stage of combustion of these shrub species is highly interesting as they are highly flammable and capable of sustaining extreme fire intensity even at moderate fire danger levels [5]. Five representative species of these communities were selected for this study: *Calluna vulgaris* (L.) Hull, *Chamaespartium tridentatum* (L.) P. Gibbs, *Erica umbellata* L., *Ulex europaeus* L. and *Ulex minor* Roth. Trying to simplify the nomenclature we name the five species as S1, S2, S3, S4 and S5, respectively.

For each species, tips of the fine ( $\phi < 6$  mm) twigs with leaves were collected in Galicia during the autumn season. Plant samples were immediately placed in plastic containers, preserving its structure. Containers were hermetically closed and brought to the laboratory, where they were stored at 5 °C to avoid water losses. Following this procedure, both fuel structure and moisture are preserved after gathered in the field and carried to the laboratory. Before each series of experiments, fuel moisture content of the selected species were determined by means of a representative sample, oven dried at 100 °C for 24 h. Table 1 presents

Table 1  
Species and moisture content

Species	Moisture content (%)
S1 ( <i>Calluna vulgaris</i> )	101
S2 ( <i>Chamaespartium tridentatum</i> )	74
S3 ( <i>Erica umbellata</i> )	74
S4 ( <i>Ulex europaeus</i> )	118
S5 ( <i>Ulex minor</i> )	105

the moisture content of each species, expressed on a dry weight percentage basis.

### 2.2. FTIR measurements

The experimental device selected to measure in situ gases emitted by thermal degradation of biomass fuel is partially based on the “flammability measurement method” developed by Delabrazze and Valette [6] to determine the flammability parameters of forest fuels. This method is fully accepted, and has widely been described [7–9].

The experimental setup is located inside of an area with a smoke evacuator working at a fixed forced draught, so that the air flow is constant. The device is composed of (see Fig. 1):

- A heating circular surface (10 cm diameter), constituted by an electric radiator powered at 300 W where samples to be tested are laid. The surface temperature is 330 °C at the steady regime. This value of temperature assures that pyrolysis processes have been completely activated.
- An artificial IR source to perform absorption measurements. This source is another electric radiator powered at 90 W. In this case, surface temperature is 140 °C. It is perpendicularly placed to the calorific focus.
- A FTIR spectrometer (FTIR-SM), working in absorption mode, located 225 cm in front of the artificial IR source.

The FTIR-SM is placed in a way that its optical line of sight is a few cm above the sample. In this way, radiation coming from the solid parts of the sample would be

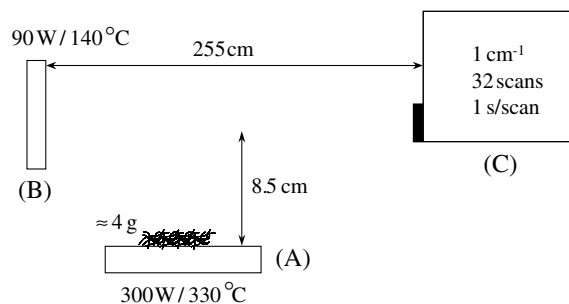


Fig. 1. Scheme of the experimental setup: (A) heating surface; (B) IR radiant source; (C) FTIR spectrometer. Distances are not critical.

avoided, and only absorption of the emitted gases would be measured. In front of the spectrometer an artificial IR source is placed to perform active remote sensing. In our experiments, the temperature of this source was 140 °C.

The use of an FTIR-SM is mandatory because of the Fourier-transform technique's advantages:

- It is necessary to perform in situ, non-intrusive measurements, avoiding manipulation of the emitted gases.
- It is necessary to measure the absorbance spectra of all the emitted gases at the same time ( Fellgett's advantage). This point is critical to compare concentrations of different gases, and it cannot be achieved by dispersive radiometers.
- It is necessary to acquire spectra fast enough to evaluate temporal evolution of gas concentrations. High acquisition speed also permits co-adding multiple scans to improve the signal-to-noise ratio.

Experimental working conditions of the FTIR-SM are also very important. Among others, two important parameters have to be carefully selected:

*Spectral resolution:* This resolution has to be good enough to determine the absorption bands. On the other hand, acquisition times have to be short enough to obtain certain information on the temporal evolution of these concentrations. Taking into account that the higher the spectral resolution, the higher the acquisition time, it is necessary to find a compromise between these two parameters. In these experiments, a spectral resolution of  $1\text{ cm}^{-1}$  has been selected as the optimum.

*Number of scans:* An appropriate number of scans has to be selected in order to guarantee a good signal-to-noise ratio and an acquisition time fast enough to obtain information on temporal evolution. In our experiments, a number of 32 scans per spectrum has been chosen.

Both spectral resolution and number of scans give an acquisition time around 30 s for each spectrum.

For each species under study, five homogeneous samples of 4 g (fresh weight) have been tested. The sample is carefully placed on the heating surface heated at 330 °C (Fig. 1), without packing it, so that its structure is quite similar to reality in the field. Thermal degradation of the sample begins to occur, and the FTIR-SM is continuously measuring the emitted gases during the process. The experiment is considered to be valid whereas no flame appears. If ignition of the sample is produced, the spectrometer will measure the energy emitted by the flame over imposed to the absorbance spectrum, giving a total spectrum meaningless. Experiments with the higher number of valid spectra have been selected as representative of each species. Fig. 2 shows an example of absorbance spectra measured for carbon dioxide and monoxide in *U. europaeus*.

### 2.3. Quantitative determination of concentrations

According to Beer's law, quantitative information could be easily obtained on the basis that intensities of spectral absorption bands are linearly proportional to the concentration of each gaseous component. However, there are different reasons that give rise to deviations from Beer's law linearity. The most important one is related to the finite spectral resolution of the acquisition system, which produces a "smoothing" of the spectrum.

A way to obtain quantitative information is to compare the experimental spectrum with other spectrum known as the reference spectrum. This one must fulfil the following items:

- Reference spectrum must have the same spectral resolution than the experimental one.
- Concentration of reference spectrum must be accurately known.

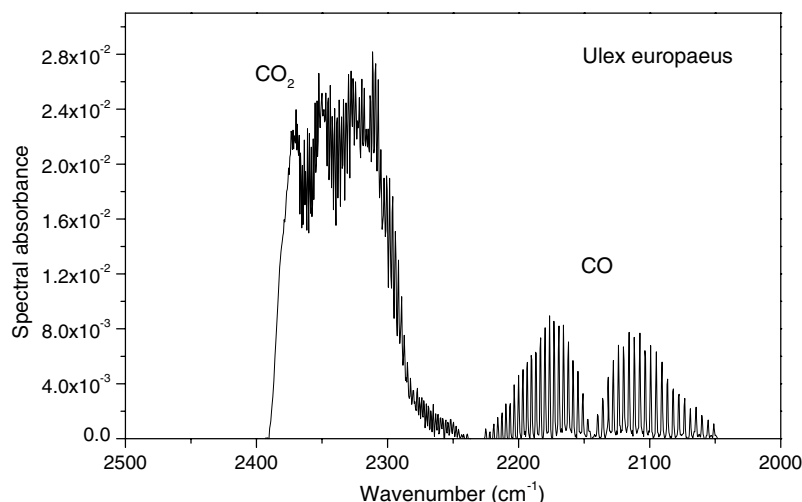


Fig. 2. Example of absorbance spectra of CO<sub>2</sub> and CO (spectral resolution  $1\text{ cm}^{-1}$ ).

- (c) Reference must be measured at a temperature as close as that of the experiment.

Multicomponent analysis procedures can provide accurate quantitative information on gas mixture when a proper set of reference spectra has been chosen (one spectrum for each different gas), by comparing it to the experimental spectrum. One of the most typical solutions for this problem is the use of classical-least-squares (CLS) regression analysis methods. The results presented in this article have been obtained from a commercial code (AUTOQUANT) that performs CLS analysis by using an advanced multivariate algorithm.

One problem to be taken into account is the fact that our experiments have been performed in open air. In these experiments, it cannot be possible to measure accurately the optical path due to the variability of the spatial location of pyrolysis gases. One solution could be to use a “chimney-like” structure to collect the emitted gases and to define a precise value of the optical path (the width of the chimney). However, this solution presents important problems related to the condensation of gases in the walls of this structure. Heating systems to solve this condensation problem makes complex the experimental setup. In order to maintain the simpler open air configuration being able to compare concentrations of different gases, we propose the use of the  $(C \times L)$  value provided by the CLS method instead of the value of  $C$ . In this work, we will call this value the “path-integrated concentration” (PIC). Units for  $C \times L$  are (parts per million meter (ppm m)). Nevertheless the optical path  $L$ , although not very well known, is not strictly necessary. In fact,  $L$  will always be the same for the different gases involved in the calculations, which is its only relevant property to be accomplished as the aim of the work is to propose a method to calculate relative concentrations of pyrolysis gases and not absolute ones.

The proposed procedure also needs to maintain a high accuracy to determine the limit of validity for quantitative analysis. One way to perform this point is to “fabricate” a set of different spectra covering a wide range of concentrations. For this purpose, a code based on the HITRAN96 spectral database has been used [10]. HITRAN is a compilation of spectroscopic parameters for 32 different molecules present in the atmosphere that a variety of computer codes use to predict and simulate the transmission and emission of light in the atmosphere.

### 3. Experimental results

#### 3.1. Carbon-related products

During the pyrolysis of biomass the most important carbon-related products are solid char and gases as  $\text{CO}_2$ ,  $\text{CO}$  and  $\text{CH}_4$  [11]. These three gases can be measured in situ by FTIR spectrometry. Table 2 shows the spectral regions used to perform the quantitative analysis.

Table 2

Spectral regions used to perform the quantitative analysis for the different gases under study

Gas	Spectral window ( $\text{cm}^{-1}$ )
Carbon monoxide	2050–2230
Carbon dioxide	2240–2400
HC	3010–3020

#### 3.1.1. $\text{CO}_2$ and $\text{CO}$ analysis

Reference spectra for  $\text{CO}_2$  and  $\text{CO}$  have been downloaded from the AEDC/EPA spectral database website [12]. They are spectra calculated using the HITRAN96 spectral database and a modified version of the fast atmospheric spectral code (FASCODE) [13]. Original spectra have been calculated at a resolution of  $0.125 \text{ cm}^{-1}$  and degraded to  $1 \text{ cm}^{-1}$  using triangle apodization.

Our proposed method states as a first step the study of the linearity limits for the use of these AEDC/EPA spectra. To do that a set of different “synthetic” spectra has been fabricated by using the HITRAN96 database and a commercial program (TRANS). This set has been analyzed by the AUTOQUANT program and the AEDC/EPA references. Fig. 3 illustrates the evaluation of the limit of validity for  $\text{CO}_2$  and  $\text{CO}$  analysis by using these reference spectra. As it can be seen, limits for the linear quantitative analysis can be identified approximately at 50 (ppm m) for  $\text{CO}_2$  and 100 (ppm m) for  $\text{CO}$ .

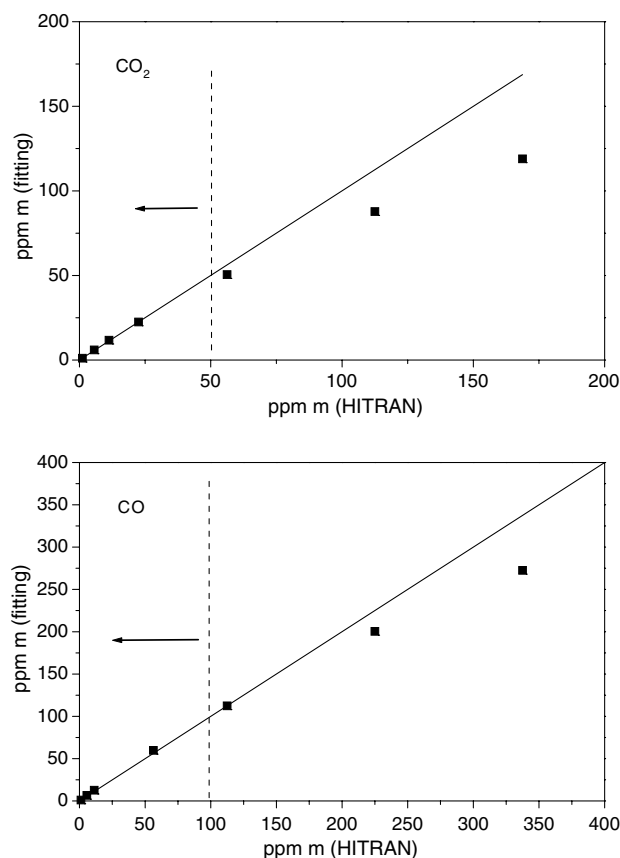


Fig. 3. Limits of validity for  $\text{CO}_2$  and  $\text{CO}$  quantitative analysis.

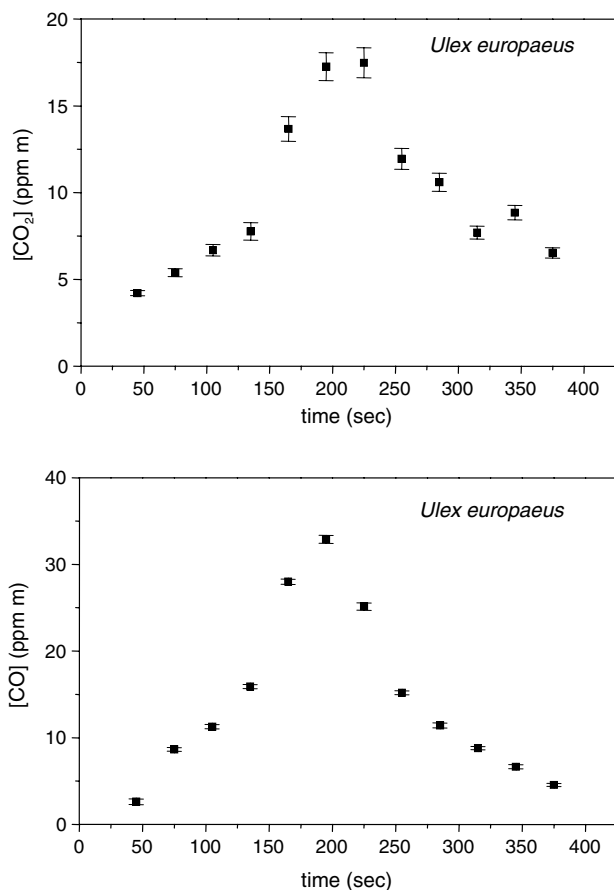


Fig. 4. Temporal evolution of path-integrated concentrations of  $\text{CO}_2$  and CO during the experimental thermal degradation of a sample S4.

Fig. 4 illustrates examples of temporal evolution of path-integrated concentration of  $\text{CO}_2$  and CO during the experimental thermal degradation of sample S4. Error bars only correspond to the error provided by the fitting subroutine of AUTOQUANT. The small value of these errors (5% for  $[\text{CO}_2]$  values and 2% for  $[\text{CO}]$  values) means that the fitting is performed satisfactorily. When quantitative analysis is performed on the whole sample set for all the species, the maximum values of path-integrated concentration never exceed the limits of validity of the method for both gases. As a conclusion, the AEDC/EPA reference spectra are valid for our purposes.

The most significant result is summarized in Fig. 5. This figure shows that  $[\text{CO}]$  correlates well with  $[\text{CO}_2] + [\text{CO}]$ . The quantity  $[\text{CO}_2] + [\text{CO}]$  represents most of the carbon released in the gas phase during the pyrolysis process. Dots represent typical results for all the species under study. The strong correlation revealed in the figure shows that the chemistry of the pyrolysis is very similar for all the tested species. Therefore, we can find a common way to describe the CO production by using this ratio

$$\frac{[\text{CO}]}{[\text{CO}_2] + [\text{CO}]} = 0.64 \pm 0.03 \quad (1)$$

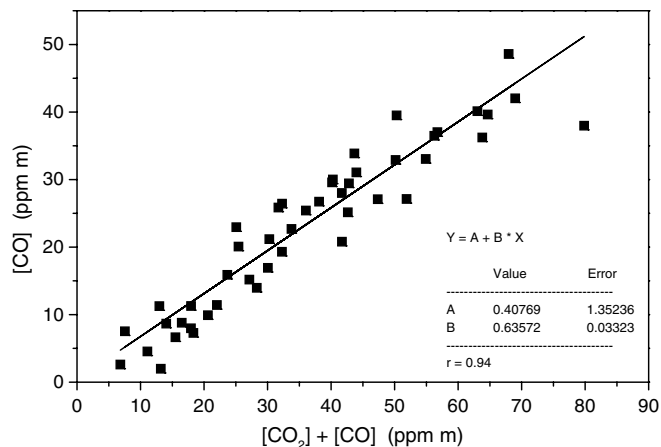


Fig. 5. CO path-integrated concentration versus an evaluation of the concentration for most of the carbon-related by-products. All the tested species are included in the plot.

This result is important, because Eq. (1) appears to be a simple and useful way to model the  $\text{CO}_2/\text{CO}$  emissions during the biomass pyrolysis process.

It is important to realize that results as showed in Fig. 5 or in Eq. (1) can be obtained because acquisition of absorbance spectra is simultaneous and the optical path  $L$  the same for both gases. These two properties are stated throughout this work for all measurements and calculations and for all involved gases. This is the reason for the use of FTIR based spectroradiometers in this kind of experiments.

### 3.1.2. $\text{CH}_4$ analysis

The study of methane absorbance spectra is not so straightforward. As can be seen in Fig. 6, a wide absorption band (typically between 2800 and 3100  $\text{cm}^{-1}$ ) superimposes the fine structure of methane. The wide band is a complex structure that corresponds mainly to the stretch of H–C bonds. This band cannot be associated to a unique compound, but it is infrared active for many hydrocarbons. Moreover, in general it is a difficult task to identify which hydrocarbon is the responsible of this band. To do that, it is necessary a commercial (and expensive) spectral database and specific software. Otherwise, to perform the quantitative analysis it is mandatory to provide pure and calibrated spectra of each component to be analyzed. That means in our case we would need (a) to identify each of the hydrocarbons contributing to the absorption band, and (b) to find calibrated spectra for each hydrocarbon. In order to avoid the need of a hydrocarbon spectral database, and taking into account that we are interested only in the methane concentration, we propose to “fabricate” a synthetic spectrum to simulate the wide band contribution. This synthetic spectrum will be included in the method as an artificial compound that will solve the overlapping between the methane band and the wide band. In order to obtain the synthetic spectrum, an experimental spectrum with only the wide absorption band and no traces of methane has

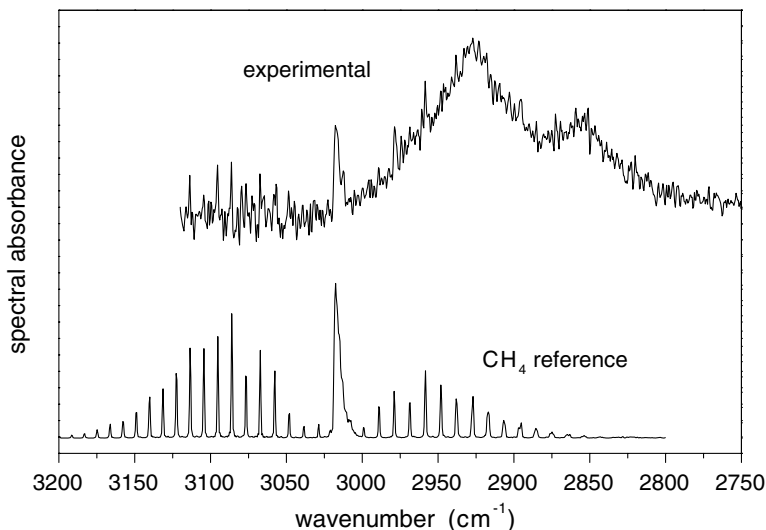


Fig. 6. (Up) Experimental absorbance band in the 2750–3150  $\text{cm}^{-1}$  spectral region. (Down) Absorbance reference spectrum for pure methane.

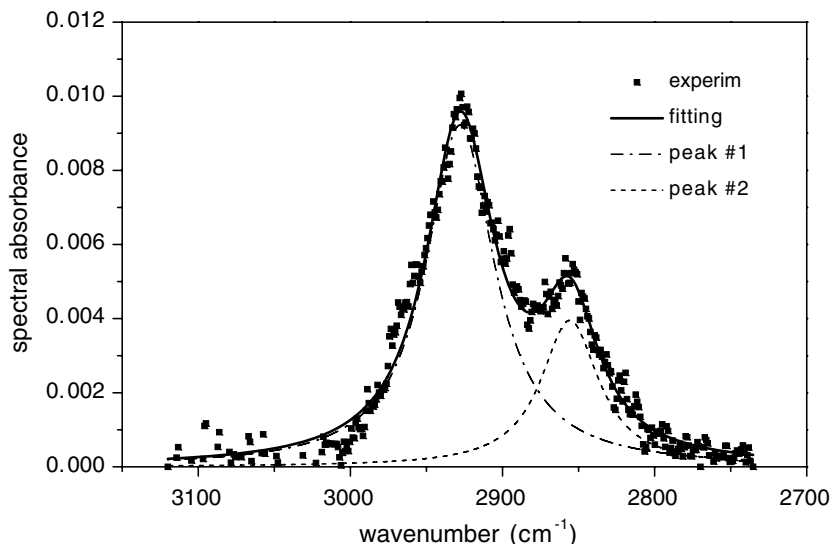


Fig. 7. Mathematical fitting of the broad absorption band corresponding to unburned hydrocarbons.

been used. An attempt to fit the wide band by using analytical equations has been performed. It has been found that the wide band has been very well fitted by the superposition of two Lorentzian functions, as can be seen in Fig. 7. This superposition will be our synthetic spectrum. Afterwards, in order to simulate experimental conditions, this synthetic spectrum has been spectrally modified by a noise function. Finally, this spectrum has been used as an artificial reference spectrum for the contribution of non-methane hydrocarbons in the quantitative analysis. Otherwise, reference spectrum for methane has been taken from the AEDC/EPA database. AUTOQUANT will use both reference spectra to separate the methane concentration values from the other hydrocarbons whichever they are. The limits of validity for the quantitative analysis have been determined as in the case of  $\text{CO}_2$  and  $\text{CO}$ . For methane, this limit has been established in 150 (ppm m). This previous analysis

gives also validity to the use of the AEDC/EPA methane reference spectrum in our study. As an example, Fig. 8 shows the temporal evolution of the path-integrated concentration for  $\text{CH}_4$  measured during the experiment with the sample S4.

In order to obtain a relative comparison of different gas emissions, a quantity called “emission ratio” is defined as the above background mixing ratio of the compound studied divided by the above mixing ratio of a reference compound. The term “mixing ratio” represents the concentration (volumetric fraction) of a gaseous compound in the atmosphere. In forest fuel burning calculations, carbon dioxide is mostly taken to be the reference compound. Emission ratios relative to  $\text{CO}_2$  are of more interpretive value than raw concentrations and remove some systematic errors [14,15]. In our work, the path-integrated concentrations have been used, and then we can obtain a path-inte-

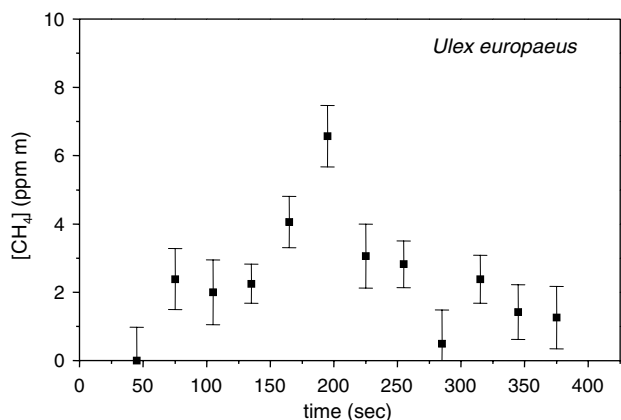


Fig. 8. Temporal evolution of path-integrated concentrations of  $\text{CH}_4$  during the experimental thermal degradation of a sample S4.

grated emission ratio (PER) by using PIC values in the definition of emission ratio.

$$\text{PER} = \frac{\text{path-integrated concentration gas}}{\text{path-integrated concentration CO}_2} \quad (2)$$

One remarkable property of PER is that provide a relative concentration between species which is independent of the optical path  $L$  used in the original measurements, so avoiding the uncertainty of its exact value. This definition allows traceability for concentration values of different species relative to  $\text{CO}_2$ , being a robust index of pyrolysis process, which is an aim for fire computer model makers.

Fig. 9 represents PER for methane versus PER for carbon monoxide. In order to compare these results with the emission of  $\text{CO}$ , an averaged value of PER for  $\text{CO}$  can be obtained from Eq. (1)

$$\text{PER}_{\text{aver}}(\text{CO}) = 1.78 \pm 0.05 \quad (3)$$

Although Fig. 9 does not show a clear linear dependence, it is possible to determine upper and lower limits for the averaged PER of  $\text{CH}_4$ . These values can be easily obtained from the slopes of the two straight lines plotted in the figure:

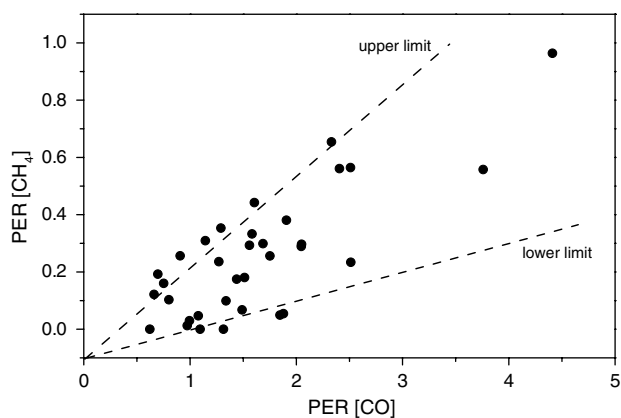


Fig. 9.  $\text{CH}_4$  path-integrated emission ratio represented as a function of  $\text{CO}$  path-integrated emission ratio. All the tested species are included in the plot.

$$\frac{\text{PER}^{\text{upp}}(\text{CH}_4)}{\text{PER}(\text{CO})} = 0.29 \quad (4)$$

$$\frac{\text{PER}^{\text{low}}(\text{CH}_4)}{\text{PER}(\text{CO})} = 0.07$$

If these values are compared with the one given by Eq. (3), it can be estimated that methane emission is roughly 20% of the values for carbon monoxide emission. Consequently, as a first approach, the influence of methane production could be neglected in a pyrolysis model.

### 3.2. Nitrogen-related products

Major nitrogen-related products of pyrolysis are nitrogen and ammonia. Nitrogen cannot be studied by infrared methods because this gas does not present any absorption band in the infrared region. On the other hand, ammonia shows absorption peaks in the  $900\text{--}975\text{ cm}^{-1}$  that can be used to obtain the path-integrated concentration of this gas.

Reference spectrum for  $\text{NH}_3$  can be downloaded from the AEDC/EPA website. The limits of validity for the quantitative analysis have been determined as in the case of  $\text{CO}_2$  and  $\text{CO}$ . For ammonia, this limit has been established in 20 (ppm m).

The quantitative method applied to ammonia absorption spectra provides the following results. Fig. 10 shows PER for ammonia versus PER for carbon monoxide. Following the same procedure as in methane analysis, it is possible to determine a straight line that takes into account an averaged behaviour for the PER values. Eq. (5) corresponds to the slope of this line

$$\frac{\text{PER}(\text{NH}_3)}{\text{PER}(\text{CO})} = 0.06 \quad (5)$$

This result indicates a low ammonia emission (6%) compared to the carbon monoxide emission. Hence, for these species, ammonia emission can also be neglected in the pyrolysis description as a first approach.

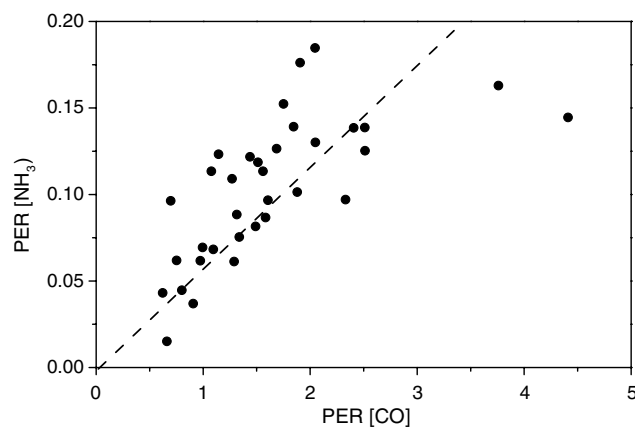


Fig. 10.  $\text{NH}_3$  path-integrated emission ratio represented as a function of  $\text{CO}$  path-integrated emission ratio. All the tested species are included in the plot.

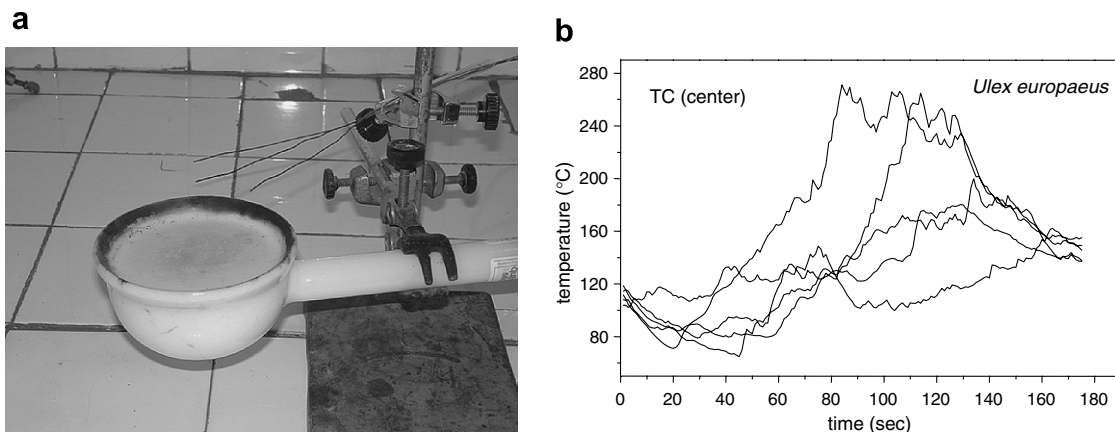


Fig. 11. (a) Thermocouple arrangement onto the radiator. (b) Temporal evolution of temperature measured by the central thermocouple during different experiments for the sample S4.

### 3.3. Temperature dependence

Temperature of pyrolysis gases plays an important role in the concentration retrieval. Absorbance at each wavenumber depends on temperature. That means that reference spectrum has to be measured/calculated at the same temperature than gases are emitted.

One important point to be determined is the temperature at which pyrolysis gases are emitted. This temperature has been measured by using three thermocouples (1 mm diameter) that define a small area located at the height intercepted by the line of sight of the FTIR-SM. Fig. 11a shows the thermocouple arrangement onto the radiator (A), and Fig. 11b illustrates a typical temporal evolution of temperature measured by the central thermocouple during one of the experiments when forest fuel was S4. As it can be seen in Fig. 11b, the temperature is far from a constant value. For sample S4 temperatures can vary between 60 °C and 260 °C. For the other species, ranges are similar. This is a very wide range that makes difficult the quantitative analysis. Problems arise when different reference spectra (one for each temperature) have to be chosen. That involves the availability of an experimental device that permits to measure at different temperatures the absorbance spectra of calibrated gas mixtures, or the use of specific software tools to calculate a set of different reference spectra depending on the temperature. In practise, it is not always possible to have reference spectra (from experiment or calculation) for a wide range of temperatures.

For practical reasons, we propose in the framework of our methodology an approach based on a temperature time average. Analysis of the different temperature curves measured for the different species will permit to define a time-averaged value of temperature. Only one reference spectrum for each gas is selected, with a temperature as close as possible to this average. For instance, average temperature in S4 gives maximum values around 150 °C. Following this criterion, reference spectra searched at AEDC/EPA database have been chosen at 400 K (the closest available temperature).

In order to evaluate the errors, two different sets of synthetic spectra have been fabricated by using the HITRAN96 spectral database; one is generated at 400 K, whereas the other is generated at 500 K. This last temperature can be considered as an upper limit at sight of temperature curves (as shown in Fig. 11b) measured in all the species. Both spectra sets have been analyzed by the AUTOQUANT method by using a reference spectrum at 400 K. In this way an estimation of errors associated to

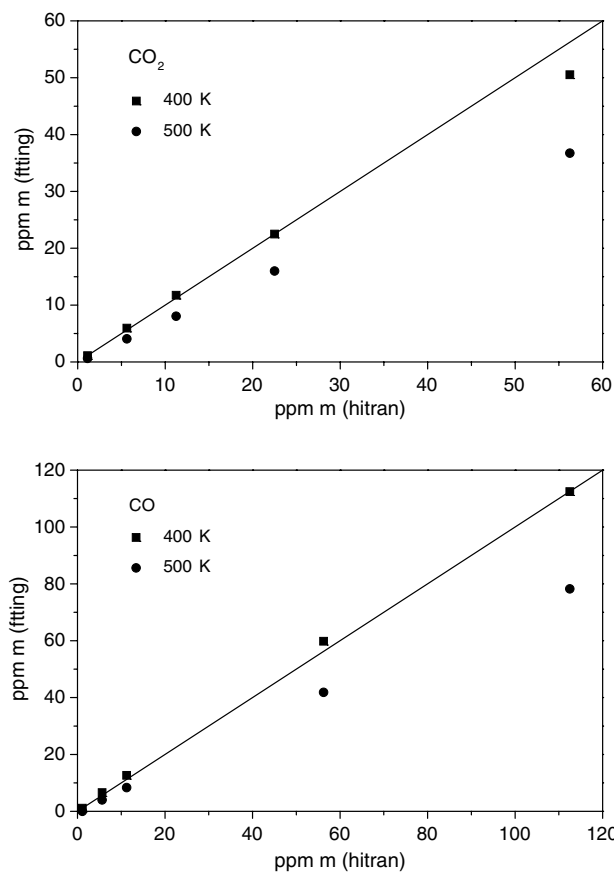


Fig. 12. Temperature dependence of the limits of validity for CO<sub>2</sub> and CO.

the use of only one reference spectrum can be calculated, at least in the range 400–500 K. Fig. 12 shows as an example results of these calculations for the most important by-products of the combustion: CO<sub>2</sub> and CO. As a summary, results from CO<sub>2</sub>, CO, CH<sub>4</sub> and NH<sub>3</sub> show that path-integrated concentration values are underestimated around a 30% when spectra at 500 K are analyzed by using references at 400 K. We consider these values as an acceptable deviation taking into account the simplicity gained by the use of one reference.

#### 4. Conclusions

From this study the most important carbon-related and nitrogen-related by-products of the pyrolysis processes in different shrub species have been measured under low heating ratio conditions. Fourier transform infrared spectrometry has been used to measure in situ the gaseous by-products of the thermal degradation process. Experiments performed at open air have been proposed in order to gain simplicity in the experimental setup. The use of path-integrated concentrations in (ppm m) is proposed to compare emission ratios from different gases. These ratios are very robust as they correspond to simultaneous measurements and independent of the optical path.

CO and CO<sub>2</sub> are by far the most important emitted gases. The chemistry of pyrolysis can be characterized in a first approximation by a simple equation, which involves CO and CO<sub>2</sub> concentrations. The most remarkable result in this work is that this main chemistry shows a common behaviour in all the species under study that can be characterized by this equation. This result can help to simplify main chemical reactions in the theoretical models of wildland fire spread.

The detection of flammable light hydrocarbons as methane is an indicator of the active pyrolysis of cellulose, as it can be seen by thermogravimetric techniques [11,16]. This active pyrolysis is mainly associated to the depolymerization of cellulose beginning at temperatures above 270 °C. In this work methane is clearly measured by the proposed method. This result is compatible with the temperature reached by the surface of the heater (330 °C). An easy way to separate methane contribution from the wide H–C absorption band for quantitative analysis is proposed by using a “synthetic” spectrum. The spectral features of this wide absorption band due to non-methane hydrocarbons are simulated quite well by using two Lorentzian curves.

Ammonia is the only nitrogen-related by-product detected in these experiments. Nitrogen oxides (NO<sub>x</sub>) are produced during the flaming combustion phase, where temperatures reach values high enough to oxidize the nitrogen [17,18]. A good degree of correlation has been measured between emission ratios for NH<sub>3</sub> and CO.

Quantitative results show that methane and ammonia emissions are roughly around 20% (CH<sub>4</sub>) and 6% (NH<sub>3</sub>)

of carbon monoxide emissions. These ratios can support a simplification in the pyrolysis models by taking into consideration only carbon monoxide and dioxide emissions.

The results exposed above can help to improve the modelling of the pyrolysis processes in physical-based models for predicting forest fire behaviour.

#### Acknowledgements

The research was funded by the European Union Project “FIRE STAR: A decision support system for fuel management and fire hazard reduction in Mediterranean wildland-urban interfaces” (Energy, Environment and Sustainable Development, Fifth Framework Programme, EVG1-CT-2001-00041). We thank the staff of Centro de Investigaciones Forestales y Ambientales de Lourizán (Xunta de Galicia), FIRE STAR partner, for collecting the plant samples used in this work.

#### References

- [1] J.M.C. Mendes-Lopes, J.M.P. Ventura, J.M.P. Amaral, Flame characteristics, temperature–time curves, and rate of spread in fires propagating in a bed of *Pinus pinaster* needles, *Int. J. Wildland Fire* 12 (1) (2003) 67–84.
- [2] F. Shafizadeh, Basic Principles of Direct Combustion, in: S.S. Sofer, O.R. Zaborsky (Eds.), *Biomass Conversion Processes for Energy and Fuels*, Plenum Publishing Corporation, New York, 1981, pp. 103–124.
- [3] R.H. White, M.A. Dietsberger, *Encyclopedia of Materials: Science and Technology*, Elsevier Science Ltd., 2001, pp. 9712–9716.
- [4] J.A. Vega, P. Cuiñas, T. Fontúrbel, P. Pérez-Gorostiaga, C. Fernández, Predicting fire behaviour in Galician (NW Spain) shrubland fuel complexes, in: *Proceedings of the III International Conference on Forest Fire Research and 14th Conference on Fire and Forest Meteorology*, vol. I, 16–20 November 1998, Luso, Portugal, pp. 713–728.
- [5] P.A.M. Fernandes, Fire spread prediction in shrub fuels in Portugal, *Forest Ecol. Manage.* 144 (2001) 67–74.
- [6] P. Delabrazé, J.C. Valette, Inflammabilité et combustibilité de la végétation forestière méditerranéenne. *Revue Forestière Française*, no. spécial Les incendies de forêts, 1974, pp. 171–177.
- [7] J.C. Valette, Inflammabilité, teneur en eau et turgescence relative de quatre espèces méditerranéennes, in: ICONA (Ed.), *Documentos del Seminario sobre Métodos y Equipos para la Prevención de Incendios Forestales*, Valencia (Spain), MAPA, Madrid, 1988, pp. 98–107.
- [8] C. Hernando, C. Moro, J.C. Valette, Flammability parameters and calorific values of *Erica arborea* and *Arbutus unedo*, in: *Proceedings of the Second International Conference on Forest Fire Research*, vol. I, 21–24 November 1994, Coimbra, Portugal, pp. 481–490.
- [9] C. Hernando, Combustibles forestales: Inflamabilidad, in: *La Defensa contra incendios forestales: Fundamentos y experiencias*, McGraw Hill, Madrid, 2000, pp. 6.3–6.15.
- [10] L.S. Rothman, C.P. Rinsland, A. Goldman, S.T. Massie, D.P. Edwards, J.M. Flaud, A. Perrin, C. Camy-Peyret, V. Dana, J.Y. Mandin, J. Schroeder, A. McCann, R.R. Gamache, R.B. Wattson, K. Yoshino, K.V. Chance, K.W. Jucks, L.R. Brown, V. Nemtchinov, P. Varanasi, *The HITRAN molecular spectroscopic database and HAWKS (HITRAN atmospheric workstation): 1996 edition*, *J. Quant. Spectrosc. Radiat. Transfer* 60 (1998) 665–710.

- [11] P.T. Williams, S. Besler, The influence of temperature and heating rate on the slow pyrolysis of biomass, *Renew. Energy* 7 (1996) 233–250.
- [12] <http://www.epa.gov/ttnemc01/ftir/welcome.html>.
- [13] H.J.P. Smith, D.J. Dube, M.E. Gardner, S.A. Clough, F.X. Kneizys, L.S. Rothman, Scientific Report 2, Air Force Geophysics Laboratory, Hanscom AFB, Massachusetts, 1978.
- [14] D.W.T. Griffith, W.G. Mankin, M.T. Coffey, D.E. Ward, A.R. Riebau, in: J.S. Levine (Ed.), *Global Biomass Burning: Atmospheric, Climatic, and Biospheric Implications*, MIT Press, Cambridge, 1991, pp. 230–239.
- [15] J.M. Lobert, D.H. Scharffe, W.M. Hao, T.A. Kuhlbusch, R. Seuwen, P. Warneck, P.J. Crutzen, in: J.S. Levine (Ed.), *Global Biomass Burning: Atmospheric, Climatic and Biosphere Implications*, MIT Press, Cambridge, 1991, pp. 289–304.
- [16] R. Basilakis, R.M. Carangelo, M.A. Wójtowicz, TG-FTIR analysis of biomass pyrolysis, *Fuel* 80 (2001) 1765–1786.
- [17] R.J. Yokelson, R.A. Susott, D.E. Ward, J. Reardon, D.W.T. Griffith, Emissions from smoldering combustion of biomass measured by open-path Fourier transform infrared spectroscopy, *J. Geophys. Res.* 102 (1997) 18865–18877.
- [18] R.J. Yokelson, D.W.T. Griffith, R.A. Susott, D.E. Ward, in: J. Greenlee (Ed.) *Perspectives on Landscape Fires*, Fairfield, WA, 1998, pp. 183–196.



本文献由“学霸图书馆-文献云下载”收集自网络，仅供学习交流使用。

学霸图书馆（www.xuebalib.com）是一个“整合众多图书馆数据库资源，提供一站式文献检索和下载服务”的24小时在线不限IP图书馆。

图书馆致力于便利、促进学习与科研，提供最强文献下载服务。

#### 图书馆导航：

[图书馆首页](#)    [文献云下载](#)    [图书馆入口](#)    [外文数据库大全](#)    [疑难文献辅助工具](#)